Quantitative measurement of the composition of $Al_xGa_{1-x}As$ heterostructures using a simple backscattered electron detector

Peter C. Sercel, John A. Lebens, and Kerry J. Vahala

Department of Applied Physics, Mail Stop 128-95, California Institute of Technology, Pasadena, California 91125

(Received 19 June 1989; accepted for publication 31 August 1989)

We describe a technique for the quantitative measurement of composition in $Al_xGa_{1-x}As$ heterostructures using a simple solid-state backscattered electron detector in a scanning electron microscope. Calibration data are presented and are shown to be consistent with the Castaing [Adv. Electron. Electron Phys. **13**, 317 (1960)] theory. The technique is applied to image representative $Al_xGa_{1-x}As$ heterostructures including a graded index separate confinement heterostructure (GRINSCH) laser structure.

INTRODUCTION

Backscattered electron (BSE) imaging in a scanning electron microscope (SEM) is a widely used technique for studying the surface topography and compositional variations of materials on a submicrometer scale.[1] In particular, the BSE signal from a sample is dependent on the atomic number Z of the elements present. As a result, imaging in the BSE detection mode provides contrast between regions of different chemical composition.[1]

BSE imaging using chemical contrast in an SEM has found use recently by investigators studying spatial compositional variations in AlGaAs epilayers.[2] The technique has certain advantages over other composition-sensitive methods. For example, BSE imaging is not limited in use to direct-gap semiconductors as is cathodoluminescence (CL), and the spatial resolution is not limited by carrier diffusion. Also BSE images can be displayed at video rates in contrast to x-ray microprobe analysis. Furthermore, compositional information is contained in the signal intensity with no necessity for spectral filtering. While several types of BSE detectors exist, the solid-state detector is particularly appealing due to its simplicity and large gain. However, in order to make quantitative measurements, the dependence of signal from the solid-state detector on the sample composition must be determined. In addition to stoichiometry, the BSE signal depends on the relative geometry of the sample, incident electron beam, and detector, as well as on the incident electron-beam energy and the energy spectrum of the backscattered electrons.

We report the development of a technique for quantitative BSE measurement of composition for samples of ternary semiconductors and apply it to the$Al_xGa_{1-x}AsAs$ system using a simple solid-state backscattered electron detector. We describe the construction of the BSE detector and present measured calibration data of backscatter signal as a function of aluminum mole fraction x. Taking into account an energy correction factor for the backscattered electrons,we show that the results are consistent with calculations employing the Castaing formula for electron backscattering coefficient of multicomponent specimens.[3,4] Finally, we present results and BSE images of two $Al_xGa_{1-x}As$ heterostructures.

I. APPARATUS

The BSE detector was fabricated by modifying a commercially available Si *p-i-n* photodetector and was mounted inside a Cambridge S-240 SEM. The detector chip is a square 500 μm on a side and is mounted inside a 2-mm-diam metal can with electrical feedthroughs to the *p-i-n* chip. The window of the casing was removed to permit an unobstructed line of sight between sample and detector. The distance between the detector and the sample was approximately 4 mm. The grounded metal can serves as a shield which prevents charging of the electrical feedthroughs and attendant image distortion. A layer of aluminum 100 nm thick was evaporated onto the surface of the detector to prevent any systematic error due to light generated in the SEM chamber. To prevent an electrical short in the detector circuit, the electrical feedthroughs were masked with a small amount of photoresist prior to the evaporation, permitting liftoff of the deposited aluminum. Due to its compactness, the detector assembly can be fixed either to the pole piece of the microscope or, more simply, to the specimen stage close to the sample. In our system, the detector is fixed to a metal arm adjacent to an optical-fiber cathodoluminescence collector described elsewhere.[5] This arrangement permits simultaneous imaging in the secondary-electron, CL, and BSE modes. The entire assembly is mounted on a three-axis motorized translation stage for convenient positioning relative to the sample.

The signal from the BSE detector is carried by shielded cable out of the SEM to a current preamp. From the preamp the signal is either routed directly to the video display electronics of the SEM or to a personal computer. The computer is equipped with standard analog-to-digital converter daughterboards for digital image storage and subsequent image-contrast enhancement. Additionally, positioning control of the electron beam can be assumed by the laboratory computer using the external beam control inputs on the

 0034-6748/89/123775-04$01.30

Cambridge SEM and standard digital-to analog converter daughterboards on the computer. This enables line scans or images to be taken with arbitrary integration time. The system is shown schematically in Fig. 1.

II. CALIBRATION OF THE BSE DETECTOR

As mentioned in the Introduction, the problem of calibration has two parts. The first concerns the dependence of the BSE signal on the geometry of the sample and detector. The second is the dependence of the BSE signal of the $Al_xGa_{1-x}As$ aluminum mole fraction x. We address the geometry issue first.

The samples examined in this study were grown by molecular-beam epitaxy (MBE) on (100) undoped GaAs substrates. The epilayers, which were undoped, ranged in aluminum mole fraction from $x = 0$ to 0.7 and were all greater than 1 μm thick. For direct-gap samples, the aluminum content was obtained from CL spectra at room temperature.[6] The aluminum mole fraction of the indirect specimens was taken from MBE-growth calibration data. The samples were cleaved and mounted in cross section for analysis. The BSE signal of the epitaxial structures was in each case measured relative to that of the GaAs substrate material—a built-in standard for each sample. In this way we expect geometrical factors to be canceled out in the determination of the relative backscatter signal of the GaAs substrate and epitaxial layers. This assumption was tested for a number of different geometries and found to be valid.

We compare our results with calculated values of the backscattering coefficient using the Castaing formula for multicomponent specimens.[3,4] According to this formula, the backscattering coefficient, defined as the ratio of total backscattered electrons to total incident electrons, of a sample with the composition $Al_xGa_{1-x}As$, is

$$\eta = \frac{xA_{Al}\eta_{Al} + (1-x)A_{Ga}\eta_{Ga} + A_{As}\eta_{As}}{xA_{Al} + (1-x)A_{Ga} + A_{As}}. \quad (1)$$

Here, A_i is the atomic weight of component i, and η_i is the backscattering coefficient of component i in its elemental form. The values of η for aluminum, gallium, and arsenic were calculated using the formula

$$\eta(Z) = 0.0254 + 0.016Z - 1.86\times10^{-4}Z^2 + 8.31\times10^{-7}Z^3, \quad (2)$$

where Z is the atomic number.[7] This formula is a fit to measurements made at normal incidence at 20 keV; however, η is approximately independent of incident electron energy between 10 and 100 keV.[7]

The gain of a solid-state detector is approximately a linear function of the energy of the detected BSE above a threshold energy which is a property of the detector.[8] Because the gain is not constant across the energy spectrum of the backscattered electrons, the detected signal is not simply proportional to the backscattering coefficient of the sample. The gain of our detector was measured as a function of electron energy by comparing the detector response to a beam of electrons normally incident on the detector to the beam current measured with a Faraday cup. The results of the gain measurement are plotted as a function of electron energy in Fig. 2. If we define $\bar{E}$ as the average energy of the backscattered electrons, the energy dependence of the signal S of the detector may then be written

$$S \propto g(\bar{E} - E_{thresh})\eta, \quad (3)$$

where g is the slope of the gain curve at $\bar{E}$, E_{thresh} is the threshold energy of the detector, and η is the backscatter coefficient of the sample under study. If $\bar{E}$ is less than E_{thresh}, the signal is taken to be zero.

In order to compare the backscattering coefficients obtained with the Castaing formula to our experimental data, we therefore need to account for any dependence of $\bar{E}$ on the sample composition. It is well known that the average energy of electrons backscattered from a material, for a given atomic number Z, increases with increasing Z.[1] To quantify this effect, we use measured values of the product $\eta\bar{E}/E_{inc}$ for silicon and gallium arsenide, for incident electron energies between 5 and 30 keV, reported in Ref. 9. The values of η for

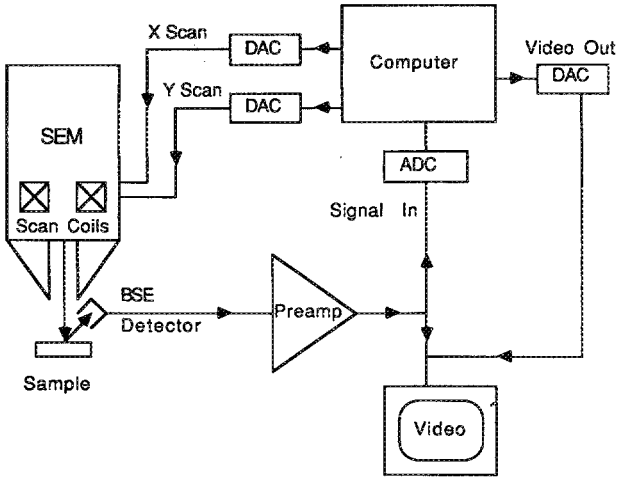

FIG. 1. Schematic diagram of BSE imaging system.

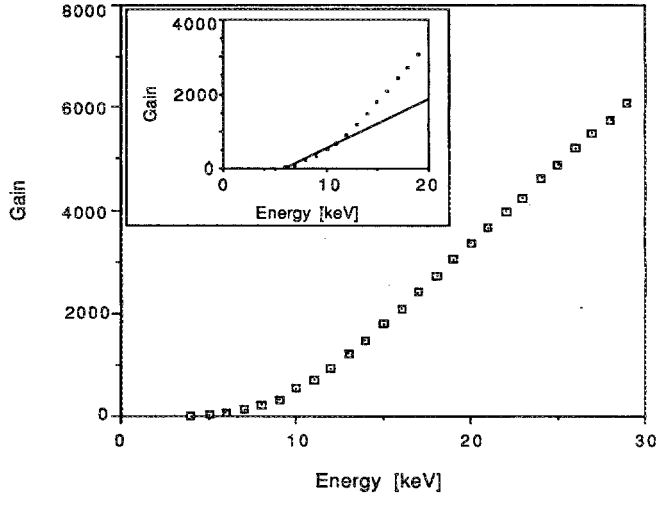

FIG. 2. Gain of the BSE detector measured as a function of electron energy. Inset: The solid line is the tangent to the gain curve at 10 keV.

Si and GaAs calculated with Eq. (1) and (2) enable us to obtain $\overline{E}$ as a function of incident electron energy for Si and GaAs. Polynomial fits to the data in Ref. 9 then give

$$\overline{E}_{\mathrm{Si}} = [0.6083 + 6.08\times10^{-3}(E_{\mathrm{inc}} - 5)]E_{\mathrm{inc}}, \tag{4}$$

$$\overline{E}_{\mathrm{GaAs}} = (0.5993 + 9.715\times10^{-3}E_{\mathrm{inc}} - 2.890\times10^{-4}E_{\mathrm{inc}}^2 + 3.990\times10^{-6}E_{\mathrm{inc}}^3)E_{\mathrm{inc}}, \tag{5}$$

where the energies are in units of keV. We then determine $\overline{E}$ for a sample of composition $Al_xGa_{1-x}As$ by interpolation in atomic number Z between silicon and gallium arsenide. To do this we employ an expression due to Everhardt in Ref. 4 for the effective atomic number Z_{eff} of a multicomponent sample. The effective Z for a sample of composition $Al_xGa_{1-x}As$ is

$$Z_{\mathrm{eff}}(x) = \frac{xZ_{\mathrm{Al}}^2 + (1-x)Z_{\mathrm{Ga}}^2 + Z_{\mathrm{As}}^2}{xZ_{\mathrm{Al}} + (1-x)Z_{\mathrm{Ga}} + Z_{\mathrm{As}}}. \tag{6}$$

The theoretical justification for this formula rests on the assumption that incident electrons lose kinetic energy continuously according to the Bethe stopping power and contribute to backscattering through single large-angle elastic collisions with the nuclei.[4]

The use of Eq. (6), and $\overline{E}$ for Si and GaAs from Eq. (4) and (5), results in the following interpolation formula for $\overline{E}$ of electrons backscattered from a sample with the composition $Al_xGa_{1-x}As$:

$$\overline{E}(x) = \overline{E}_{\mathrm{Si}} + \frac{\overline{E}_{\mathrm{GaAs}} - \overline{E}_{\mathrm{Si}}}{Z_{\mathrm{eff}}(0) - 14}[Z_{\mathrm{eff}}(x) - 14]. \tag{7}$$

We can now obtain values of the backscatter coefficient for our calibration samples. Using Eqs. (3) and (7), we find that the backscatter coefficient of $Al_xGa_{1-x}As$ as a function of aluminum mole fraction x is

$$\eta(x) = \frac{S(x)[\overline{E}(x) - E_{\mathrm{thresh}}]}{S(0)[\overline{E}(0) - E_{\mathrm{thresh}}]}\eta_{\mathrm{GaAs}}, \tag{8}$$

where $S(x)$ is the measured BSE signal from the AlGaAs epilayer, $S(0)$ is the BSE signal from the GaAs substrate, and $\overline{E}(0)$ is the average energy of BSE from GaAs calculated with (5). The value of E_{thresh} is obtained as the energy intercept of the tangent to the gain curve $G(E)$ at the point $\overline{E}$. For this discussion the incident electron energy used was 15 keV; so $\overline{E}\sim10$ keV and $E_{\mathrm{thresh}}\sim6$ keV. A 15-keV beam was chosen in order to maximize the spatial resolution of the BSE images while preserving a reasonable signal level. Values of η determined from experimental data in this way are plotted as a function of aluminum mole fraction x, along with the theoretical curve using the Castaing formula (1), in Fig. 3.

We see that the data in Fig. 3 agree well with the theoretical curve. Calibration data taken at higher incident electron energies give equally good fits to the Castaing formula when the energy dependence of the backscattered electrons is accounted for according to Eq. (7) and the detector parameter E_{thresh} determined as described above. Equations (8) and (1) can therefore be used iteratively to calculate the aluminum mole fraction x, of an epilayer with composition $Al_xGa_{1-x}As$, given the measured value of its BSE signal relative to a GaAs substrate.

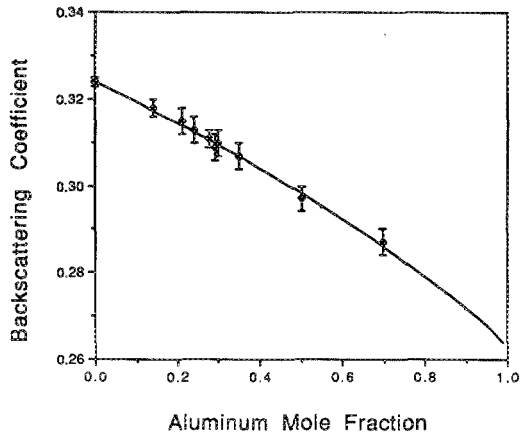

FIG. 3. Backscattering coefficient for $Al_xGa_{1-x}As$ as a function of aluminum mole fraction x. The points are experimental values obtained from measured backscatter signal using Eq. (8). The solid line is generated using the Castaing formula (1).

III. APPLICATION

To demonstrate the sensitivity and spatial resolution of our BSE imaging system, we studied two samples. The first is an MBE growth of undoped AlGaAs layers on an undoped GaAs substrate in the following order: 50 nm AlAs; 1.0 μm

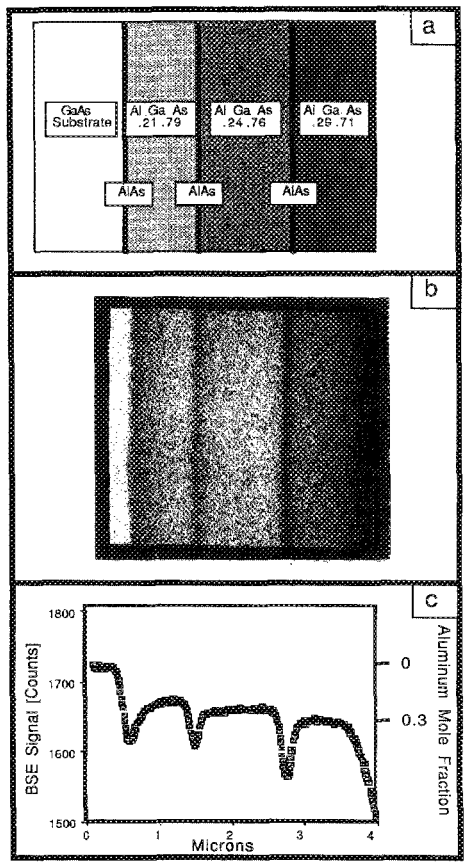

FIG. 4. (a) Schematic diagram of layered structure described in text. (b) Contrast-enhanced BSE image of layered structure described in the text. The image is of a cross section. The left part of the image is the GaAs substrate. (c) BSE line scan of same structure as (a). The left side is the GaAs substrate. The signal decreases with increasing Al content.

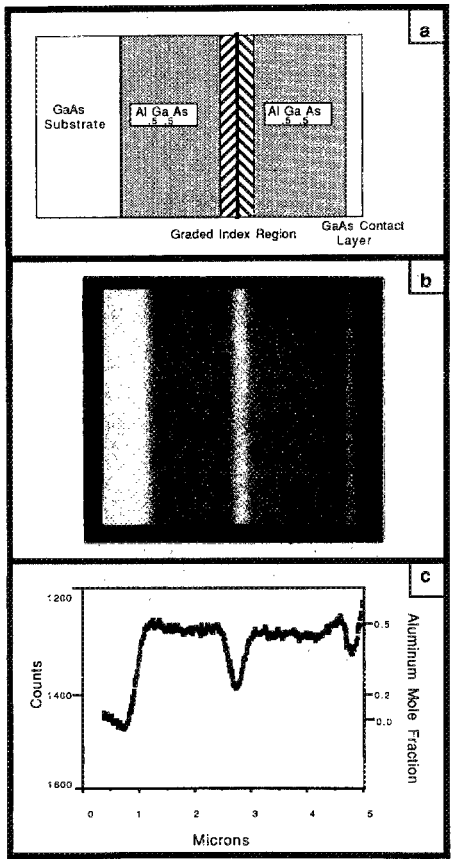

FIG. 5. (a) Schematic diagram of GRINSCH laser structure. $Al_xGa_{1-x}As$ aluminum mole fraction x is plotted vs growth direction from the substrate. (b) Contrast-enhanced BSE image of the GRINSCH laser structure. The GaAs substrate is at the left of the picture. (c) BSE line scan of GRINSCH structure shown in (b). The left side is the GaAs substrate. The signal decreases with increasing Al content.

$Al_{0.29}Ga_{0.71}As$; 50 nm AlAs; 1.3 μm $Al_{0.24}Ga_{0.76}As$; 50 nm AlAs; 1.1 μm $Al_{0.21}Ga_{0.79}As$. A schematic drawing of this sample appears in Fig. 4(a). Figure 4(b) shows a contrast-enhanced BSE image of this structure in cross section. In it the AlAs layers are visible, and the contrast due to composition differences among the AlGaAs layers is clear. In Fig. 4(c) is a BSE line scan across the layers, showing BSE signal as a function of position across the cleave. We see that the 50-nm AlAs layers are not fully resolved. This is due to the lateral spreading of the electron beam due to elastic scattering as it penetrates the sample. The signal corresponding to the AlAs layers therefore represents a convolution of the layer structure and the interaction volume of the electron beam, as is discussed in Ref. 4. Note that the small difference in aluminum mole fraction x among the AlGaAs layers is easily determined with the BSE line scan.

Figure 5(a) shows a schematic diagram of a graded index separate confinement heterostructure (GRINSCH) laser structure.[10] In Fig. 5(b) we show a contrast-enhanced image of the GRINSCH structure in cross section taken with our BSE detector. The GaAs contact layer, the AlGaAs cladding, the graded index region, and the GaAs substrate are clearly resolved. Figure 5(c) shows a BSE line scan of the same sample. We note the signal rolloff near the edge of the sample which is due to electrons scattering out of the sample near the edge. The graded index region, which is 400 nm thick, shows up clearly, as does the 300-nm GaAs contact region.

ACKNOWLEDGMENTS

The authors would like to thank Lars Eng for supplying MBE material and growth calibration data. This work was supported by the Office of Naval Research and SDIO-ISTC.P.C.S. would like to acknowledge support under a NSF Graduate Fellowship.

[1] L. Reimer, *Scanning Electron Microscopy* (Springer, Berlin, 1985), Chap.6.
[2] E. Kapon, J. P. Harbison, C. P. Yun, and L. T. Florez, Appl. Phys. Lett. **54**, 304 (1989).
[3] R. Castaing, Adv. Electron Electron Phys. **13**, 317 (1960).
[4] R. Herrmann and L. Reimer, Scanning **6**, 20 (1984).
[5] M. E. Hoenk and K. J. Vahala, Rev. Sci. Instrum. **60**, 226 (1989).
[6] H. C. Casey, Jr. and M. B. Panish, *Heterostructure Lasers* (Academic, New York, 1978), Pts. A and B.
[7] L. Reimer, *Scanning Electron Microscopy* (Springer, Berlin, 1985), p. 137.
[8] L. Reimer, *Scanning Electron Microscopy* (Springer, Berlin, 1985), Chap. 5.
[9] C. J. Wu and D. B. Wittry, J. Appl. Phys. **49**, 2827 (1978).
[10] W. T. Tsang, Appl. Phys. Lett. **39**, 134 (1989).